Experiments for Convolution Sparse Coding using alphacsc Library

Dina EL ZEIN dina.el-zein@ens-lyon.fr
Romy BEAUTÉ romy.beaute@ens.psl.eu

April 1, 2022

Abstract

This report is based on an article entitled Multivariate Convolutional Sparse Coding for Electromagnetic Brain Signals [11] in which they propose an approach for electromagnetic neural signals to analyze the waveforms that cannot be analyzed by linear filters and traditional signal representations. The approach uses a multivariate convolutional sparse coding (CSC) algorithms and imposes a rank-1 constraint on the atoms to improve the estimation of patterns as well as the separation of overlapping sources. By developing a complementary method to classical statistical analysis of complex data, this approach presents a twofold advantage when applied to neural time series. First, we will show that this approach helps capturing neural oscillatory dynamics by studying transient events as well as waveform symmetry. Secondly, we explain how it favours a more efficient computation and a better neurophysiological interpretation, as it allows a more comprehensive association of the signal patterns with their (spatial) origin in the brain.

1 Introduction

Scientific context of the article. Neural signal exhibit diverse and complex morphologies [7]. The rhythmic nature of neural activity (brain waves), and its causal or epiphenomenal role in cognitive functions is still a highly debated question [8]. Descriptions and quantification of neural activity have largely relied on standard signal processing methodologies that decompose the signal into sinusoidal components [1] and average it in the spectral domain [10], leading to the weak assumption that brain waves are rhythmically sustained. However, recent works have pointed out the need for extended methods that can better capture oscillatory dynamics, such that the morphology of waveform and the study of transient events, by accounting for the nonsinusoidal and non-stationary behavior of neural signal [1]. Indeed, classical representation methods and linear filters do not enable performing more fine-grained analysis of complex signal representation. Using multivariate convolutional sparse coding algorithms, [11] present a twofold advance for learning more complex and precise representation for multivariate signal, while allowing to associate spatial patterns to their origin in the brain. It is important to stress that this last point is directly related to the need to take into consideration the physiological and physical properties of the data acquired from a specific (neuroimaging) method, in this case magnetoencephalography (MEG) and electroencephalography (EEG). Due to physical properties such as cranial conduction, electromagnetic signals are scattered in the brain, making it difficult to assess the origin of the signal from the raw signal. The instantaneousness and linearity of the spreading of neural activity can be modelled using Maxwell's equations [6], and imply that similar time patterns with different intensities - relative to the origin of the signal - will be

recorded on each channel. To account for the linear and instantaneous spreading properties of the signal over the scalp, a $rank - 1$ constraint is applied on the atoms.

Contribution of the article. Using Maxwell's equation properties and physical model of electrophysiological signals (linearity forward model), [11] designed a multivariate model for CSC consists in imposing a $rank - 1$ constraint on each dictionary of multivariate spatio-temporal atoms (P channels x L atoms). Furthermore, they proposed a locally greedy coordinate descent (LGCD) [9] and precomputation steps strategies to gain in efficiency and rapidity in the optimization part. All together, this method extends the classical approaches to the case of multivariate signals while considering the properties of the signal through a rank-1 constraint, and allows a faster, more efficient, and more accurate estimation of neural patterns and their origin in the brain 1.

Implementation, extension & contribution to the article. In this study, we will perform and present the following extensions regarding:

1. Evaluation of the efficiency of the proposed LGCD algorithm using rank-1 constraint, and comparing it when dropping the rank-1 on the MNE sample [1] data. By comparing the efficiency of the implementation on a new experimental dataset with and without the rank-1 constraint, we show the added value of this approach for automatically learning brain waveforms atoms. Second, performing an analysis on the MNE sample[1] allows formulating a neuroscientific interpretation of the learned atoms with respect to the experimental condition, as this dataset contains stimuli from different modalities i.e. visual and auditory.
2. Present a comparison for speed performance between different CSC approaches for univariate signal mainly: (1) CBPDN [2], (2) Fista [7], (3) LBFGS [7], (4) the proposed LGCD [11]; and for multivariate signals: (1) CBPDN [13], the proposed LGCD [11] with full rank and with rank-1 constraint on the MNE sample data[1].

The experiments were all done in Python and available at https://github.com/dinalzein/CSC.

2 Method

2.1 CSC Approaches

Univariate CSC. Given a univariate signal $\{\mathbf{x^n}\}_{\mathbf{n=1}}^{\mathbf{N}} \subset \mathbb{R}^T$ (T is time points) with N observed signals, the convolutional sparse coding task amounts to solve the following optimization problem:

$$\min_{\{\mathbf{d}_k\}_k, \{\mathbf{z}_k^n\}_{k,n} \|\mathbf{d}_k\|^2 \leq 1} \sum_{n=1}^{N} \frac{1}{2} \left\| \mathbf{x^n} - \sum_{k=1}^{K} \mathbf{z}_k^n * \mathbf{d}_k \right\|_2^2 + \lambda \sum_{k=1}^{K} \|\mathbf{z}_k^n\|_1 \tag{1}$$

where $\{d\}_{k=1}^K \subset \mathbb{R}^L$ (L is times atoms) are the K temporal atoms (patterns) that we aim to learn, and $\{z_k^n\}_{k=1}^K \in \mathbb{R}^{N-L+1}$ are K activations signals, and $\lambda > 0$ is the sparsity constraint.

This optimization problem comes to minimizing a ℓ_2 reconstruction loss, corresponding to a Gaussian noise model associated with a sparsity-inducing ℓ_1 penalty term.

[1] https://mne.tools/dev/generated/mne.datasets.sample.data_path.html

Multivariate CSC. For multivariate signals $\{\mathbf{X^n}\}_{\mathbf{n=1}}^{\mathbf{N}} \subset \mathbb{R}^{P\times T}$ with N observed multivariate recorded over P channels, the convolutional sparse coding task amounts to solve the following optimization problem:

$$\min_{\{\mathbf{D}_k\}_k, \{\mathbf{z}_k^n\}_{k,n} \|\mathbf{D}_k\|_2^2 \leq 1, z_k^n \geq 0} \sum_{n=1}^{N} \frac{1}{2} \quad \left\| \mathbf{X^n} - \sum_{k=1}^{K} \mathbf{z}_k^n * \mathbf{D}_k \right\|_2^2 \quad + \quad \lambda \sum_{k=1}^{K} \|\mathbf{z}_k^n\|_1 \tag{2}$$

where $\{D\}_{k=1}^{K} \subset \mathbb{R}^{P\times L}$ are the K spatio-temporal atoms (patterns) that we aim to learn, and $\{z_k^n\}_{k=1}^{K} \in \mathbb{R}^{N-L+1}$ are the sparse activations associated with X^n, and $\lambda > 0$ is the sparsity constraint.

Multivariate CSC with rank-1 constraint. Physical properties making the electromagnetic waves - recorded from magnetoencephalography (MEG) - propagating instantaneously and adding up linearly led to extend multivariate CSC models by adding a rank-1 constraint, meaningful in terms of neuroscientific interpretation . Here, the multivariate CSC model is threfore extended with an additional constraint on the multivariate atoms that have to be rank-1. Each atom might be written as a product of univariate vectors $D_k = u_k v_k^\top$, where $u_k^\top \in \mathbb{R}^P$ is the pattern over channels, and $v_k^\top \in \mathbb{R}^L$ is the pattern over time. The objective function is formalized as follow :

$$\min_{\{\mathbf{u}_k\}_k, \{\mathbf{v}_k\}_k, \{\mathbf{z}_k^n\}_{k,n}} \sum_{n=1}^{N} \frac{1}{2} \quad \left\| \mathbf{X^n} - \sum_{k=1}^{K} \mathbf{z}_k^n * (\mathbf{u}_k \mathbf{v}_k^T) \right\|_2^2 \quad + \quad \lambda \sum_{k=1}^{K} \|\mathbf{z}_k^n\|_1 \tag{3}$$

such that $\|\mathbf{u}_k\|_2^2 \leq 1, \|\mathbf{v}_k\|_2^2 \leq 1, \text{and} z_k^n \geq 0$

2.2 Model Estimation

All of these three problems are convex in each variable alone but not jointly convex. Thus the solution depends on the initialization.
In this section, we focus on the multivariate CSC with rank-1 constraint 3 and present the approach of [11] which is done using a block coordinate descent approach that minimizes alternately the objective function over the activations z_n^k, the spatial patterns u_k, and the temporal pattern v_k.

Z-step:solving for the activations. The goal of the Z-step is to get the NK activation signals given K fixed atoms D_k and the regularization parameter λ. This problem is convex and can be solved using proposed algorithms based on ADMM [2], FISTA [7], and L-BFGS [7] yet these algorithms can be slow on large signals due to the computation of the gradient. For this, a locally greedy coordinate descent (LGCD) strategy is used to reduce the cost of gradient computation [9]. It updates the estimate solution for $z_k[t]$ one coordinate at a time chosen greedily in one of M subsegments of the signal. A pseudo-code of LGCD algorithm is displayed in Figure 5 in the appendix.

D-step: solving for the atoms. The D-step aims to update K spatial patterns u_k and K temporal patterns v_k given KN fixed activation signals z_k^n. The problem here is convex in each block of variables $\{u_k\}_k$ and $\{v_k\}_k$, but not jointly convex. Thus, it is optimized over one variable at time using a projected gradient descent with an Armijo backtracking line-search [14].

3 Data

Sample data[1]: neuroscientific interpretation of learn atoms. The data used in the original article, somatosensory data [2], contains MEG recordings of one patient's responses to median nerve stimulation, and is available on the MNE software [4, 5]. In this work, we use a different data, sample[1] that contains MEG and EEG recordings from one subject performing an audiovisual experiment. We applied the following pre-processing procedure :

- We resampled the signal with a sampling frequency of $150Hz$ to limit the computational complexity;
- $P = 203$ gradiometer channels were used and preprocessed using a notch filter at $60Hz$ to reduce powerline (noise) artifacts, a lowpass filter at $75Hz$ as well as a highpass filter at $2Hz$ to remove low frequency trend (drift artifacts largely contribute to the raw signal variance);
- Data was loaded as an array and split in (independant) chunks for parallelization during the model fit. The apply_window parameter was set to True to limit the impact of border artifacts.

The experimental part of this dataset consist in presenting the subject with checkerboard patterns in the left and right visual field, interspersed with tones in the left or right ear. From time to time, a smiling face was presented in the centre of the visual field, and the subject was asked to press a key with the right index finger as soon as possible after the face appeared. An index number was associated to characterise response to stimuli given its modality (auditory/visual) and laterality (right/left). Note that making use of stimuli from different nature will enable us to determine if the learnt atoms are consistent with the modality and laterality of a given stimuli. The stimulations event were described and stored in a dictionary to be able to extract epochs corresponding to the different events from the continuous data recording.

4 Results

Comparison of recovery performance with and without rank-1 constraint. The original paper [11] showed that we can retrieve the neural sources of the learned atoms, and that these sources are coherent with the brain regions known to be activated for the given task (when using MNE Somatosensory data[2]). With our experiments on the sample data [1], we try to see if we can establish a correspondance between the localization of the learned atoms and the nature of the presented stimuli, in terms of modality and lateralization as this dataset contains data for auditory and visual stimuli. Our hypothesis is the following: the atoms learned from the "visual" epochs should localize around occipital areas, while the ones learned from the "auditory" ones should localize more around temporal regions.

We present the results of the proposed algorithm on the sample data[1] after applying a preprocessing procedure presented in Section 3. We learned $K = 40$ atoms with $L = 1000$ ms using a rank-1 multivariate CSC model with a regularization $\lambda = 0.1$. Figure 2 in appendix shows the results of this experiment. In terms of neuroscientific interpretation, the temporal pattern associated with atom 0 shows a heartbeat artifact. It is well recognizable by its QRS [3] components that represents the spread of a stimulus through the ventricles [3]. The spatial pattern associated

[2] https://mne.tools/stable/generated/mne.datasets.somato.data_path.html

[3] Quartz Rate Sensor

	CBPDN [2]	Fista [7]	LBFGS [7]	LGCD[11]
$\lambda = 0.3$	20	13	75	480
$\lambda = 1.$	70	165	142	320
$\lambda = 3.$	90	157	170	190
$\lambda = 10.$	110	148	175	80

Table 1: Time in sec to reach a precision of 0.01 using the state-of-the-art CSC solvers for univariate signals.

to this event is represented outside of the scalp, as the origin of this signal is further away from the source of measurement. The spatial and temporal patterns associated with atom 1 represent the recovery of blink artifacts. The spatial and temporal patterns associated with atom 2 seems to correspond to a bilateral regions inside the brain, which could be consistent considering the alternance of laterality (right/left) of the task events. Furthermore, the rank-1 nature of the atoms learnt by the proposed algorithm justifies fitting an equivalent current dipole to better infer the real source of the signal[12].

To show the competitively of the proposed algorithm, we replicated the same experiment but with dropping the rank-1 constraint. The results from Figure 4 (appendix) show that the rank-1 constraint enabled a better neuroscientific interpretation of the learn atoms. Indeed, we see from Figure 4 that the recovery of neurologically plausible atoms is very limited, as the patterns are very noisy and that neuroscientific interpretation (i.e. origins in the brain, and neural events accounting for cognitive processing) can be hardly established .

The results of this experiment can be replicated using LGCD_rank1_experiments.ipynb in the github repository [4].

Speed performance of CSC solvers. We use the sample data[1] to measure the performance of different state-of-the-art CSC algorithms on both univariate and multivariate signals. Though all algorithms have the same objective function and share the same initial setting, it is not guaranteed to reach the same local minima as the problem is non-convex. We consider the following values for parameters: $L = 128$, $K = 8$, and $\lambda = [0.3, 1., 3., 10.]$. For univariate CSC solvers, we compare the proposed algorithm against CBPDN developed by [2] and both Fista and LBFGS developed by [7]. The results are presented in Table 1 and show that the proposed algorithm is very efficient for sparse activations (results on this data are coherent with the paper).

For multivariate CSC solvers, we compare the proposed LGCD with full rank and with rank-1 constraint againt CBPDN [13] with $P = 5$ channels. The results are presented in Table 2and show rank-1 constraint has better performance over the full rank approach but does not over-perform CBPDN [13]. In [11], CBPDN [13] outperform the proposed LGCD with rank-1 using MNE Somatosensory [2] data with sparse activations.

The results of this experiment can be replicated using comparison_of_CSC_solvers.ipynb in the github repository[4]

[4] https://github.com/dinalzein/CSC

	CBPDN [13]	LGCD full rank [11]	LGCD rank-1 [11]
$\lambda = 0.3$	40	168	135
$\lambda = 1.$	57	145	125
$\lambda = 3.$	61	122	115
$\lambda = 10.$	60	50	82

Table 2: Time in sec to reach a precision of 0.01 using the state-of-the-art CSC solvers for multivariate signals.

5 Conclusion

In this work, we conducted supplementary analysis and experiments to evaluate the performance of the proposed LGCD with rank-1 algorithm. The experiments were done on a new dataset, sample [1], that has stimuli of different modalities. We showed the added value of the rank-1 constraint on the LGCD algorithm in terms of reconstructed atoms. Our results encourage to keep comparing the performance of this model on datasets involving different experimental conditions, to determine if the atoms learnt using the LGCD with rank-1 constraint approach indeed can recover neurologically plausible atoms depending on the experimental conditions.

References

[1] Scott Cole and Bradley Voytek. "Cycle-by-cycle analysis of neural oscillations". In: (Apr. 2018). DOI: 10.1101/302000. URL: https://doi.org/10.1101/302000.

[2] Cristina Garcia-Cardona and Brendt Wohlberg. "Convolutional dictionary learning: A comparative review and new algorithms". In: *IEEE Transactions on Computational Imaging* 4.3 (2018), pp. 366–381.

[3] Ary L Goldberger, Zachary D Goldberger, and Alexei Shvilkin. "Chapter 3: How to Make Basic ECG Measurements". In: *Goldberger's Clinical Electrocardiography (Ninth Edition): Elsevier* (2018), pp. 11–20.

[4] Alexandre Gramfort. "MEG and EEG data analysis with MNE-Python". In: *Frontiers in Neuroscience* 7 (2013). DOI: 10.3389/fnins.2013.00267. URL: https://doi.org/10.3389/fnins.2013.00267.

[5] Alexandre Gramfort et al. "MNE software for processing MEG and EEG data". In: *Neuroimage* 86 (2014), pp. 446–460.

[6] Riitta Hari and Aina Puce. *MEG-EEG Primer*. Oxford University Press, 2017.

[7] Mainak Jas et al. *Learning the Morphology of Brain Signals Using Alpha-Stable Convolutional Sparse Coding*. 2017. arXiv: 1705.08006 [stat.ML].

[8] Stephanie R Jones. "When brain rhythms aren't 'rhythmic': implication for their mechanisms and meaning". In: *Current Opinion in Neurobiology* 40 (Oct. 2016), pp. 72–80. DOI: 10.1016/j.conb.2016.06.010. URL: https://doi.org/10.1016/j.conb.2016.06.010.

[9] Thomas Moreau, Laurent Oudre, and Nicolas Vayatis. "Dicod: Distributed convolutional coordinate descent for convolutional sparse coding". In: *International Conference on Machine Learning*. PMLR. 2018, pp. 3626–3634.

[10] C Tallon-Baudry. "Oscillatory gamma activity in humans and its role in object representation". In: *Trends in Cognitive Sciences* 3.4 (Apr. 1999), pp. 151–162. DOI: 10.1016/s1364-6613(99)01299-1. URL: https://doi.org/10.1016/s1364-6613(99)01299-1.

[11] Tom Dupré La Tour et al. *Multivariate Convolutional Sparse Coding for Electromagnetic Brain Signals*. 2018. arXiv: 1805.09654 [eess.SP].

[12] T Tuomisto et al. "Studies of auditory evoked magnetic and electric responses: Modality specificity and modelling". In: *Il Nuovo Cimento D* 2.2 (1983), pp. 471–483.

[13] Brendt Wohlberg. "Convolutional sparse representation of color images". In: *2016 IEEE Southwest Symposium on Image Analysis and Interpretation (SSIAI)*. IEEE. 2016, pp. 57–60.

[14] Stephen Wright, Jorge Nocedal, et al. "Numerical optimization". In: *Springer Science* 35.67-68 (1999), p. 7.

6 Appendix

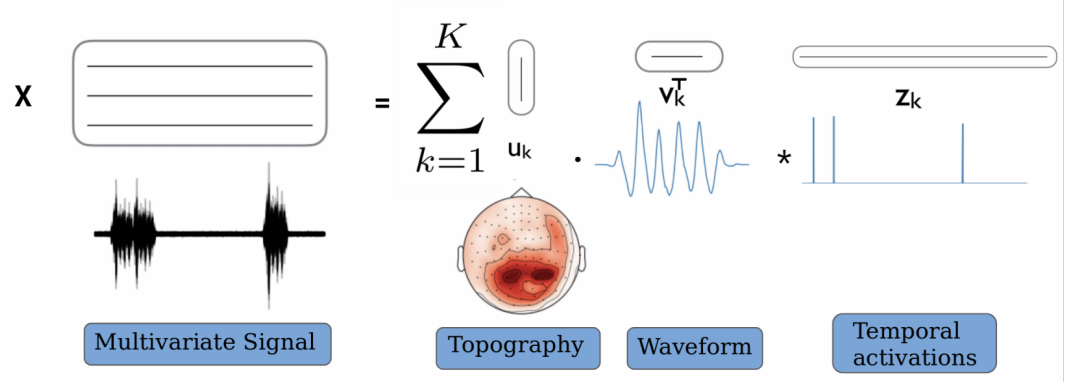

Figure 1: Illustration of the rank-1 Convolutional Sparse Coding (CSC) model showing: the K Temporal activations z_k^n associated to each signal, the Topography refers to the spatial patterns u_k, and the Waveform refers to the temporal pattern v_k.

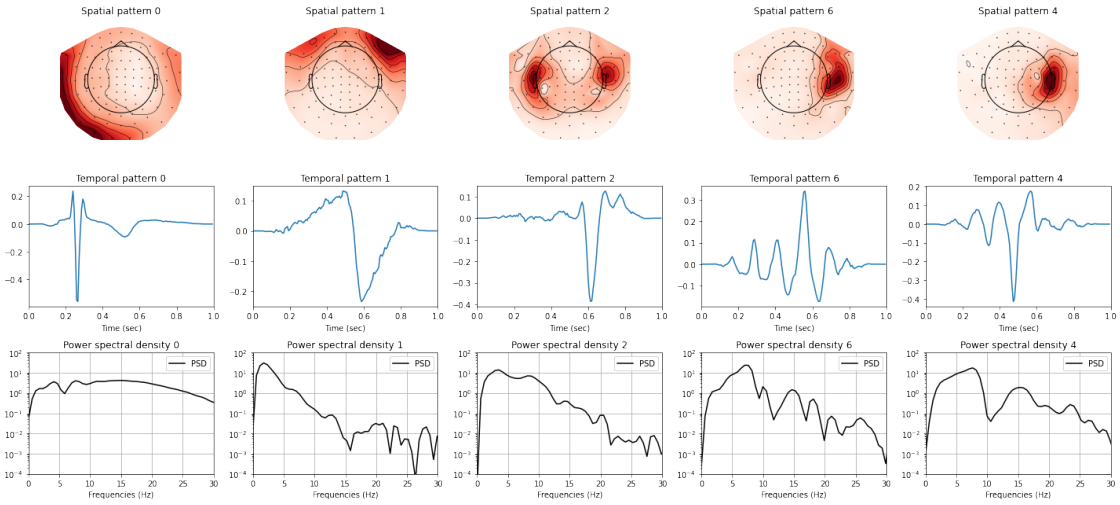

Figure 2: The figure represents the results obtained after learning atoms **with rank-1 constraint** on the sample dataset [1]. The first row shows the spatial pattern of the 5 preselected atoms of interest, i.e. atoms that are mapped on top of the sensors. The middle row display the temporal pattern of these preselected atom. The last row displays the power spectral density (PSD). In terms of neuroscientific interpretation, the temporal pattern associated with atom 0 shows a heartbeat artefact. It is well recognizable by its QRS components that represents the spread of a stimulus through the ventricles [3]. The spatial pattern associated to this event is represented outside of the scalp, as the origin of this signal is further away from the source of measurement. The spatial and temporal patterns associated with atom 1 represent the recovery of blink artefacts. The spatial and temporal patterns associated with atom 2 seem to correspond to a bilateral regions inside the brain, which could be consistent considering the alternance of laterality (right/left) of the task events.

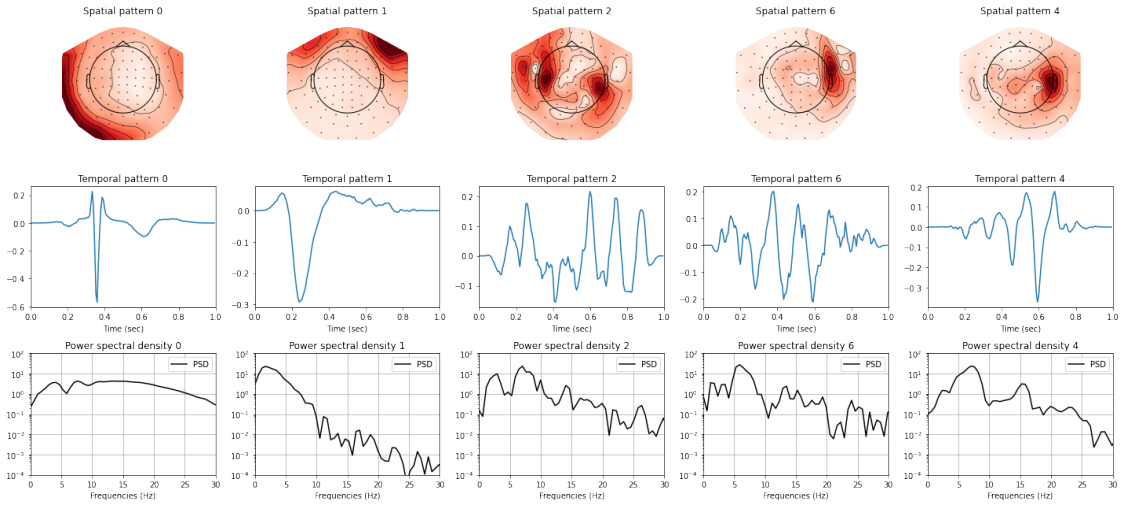

Figure 3: The figure represents the results obtained after learning atoms **without the rank1 constraint** on the sample dataset [1]. The first row shows the spatial pattern (map) of the 5 pre-selected atoms of interest. The second row displays the temporal pattern of these preselected atom. The last row displays the power spectral density (PSD).

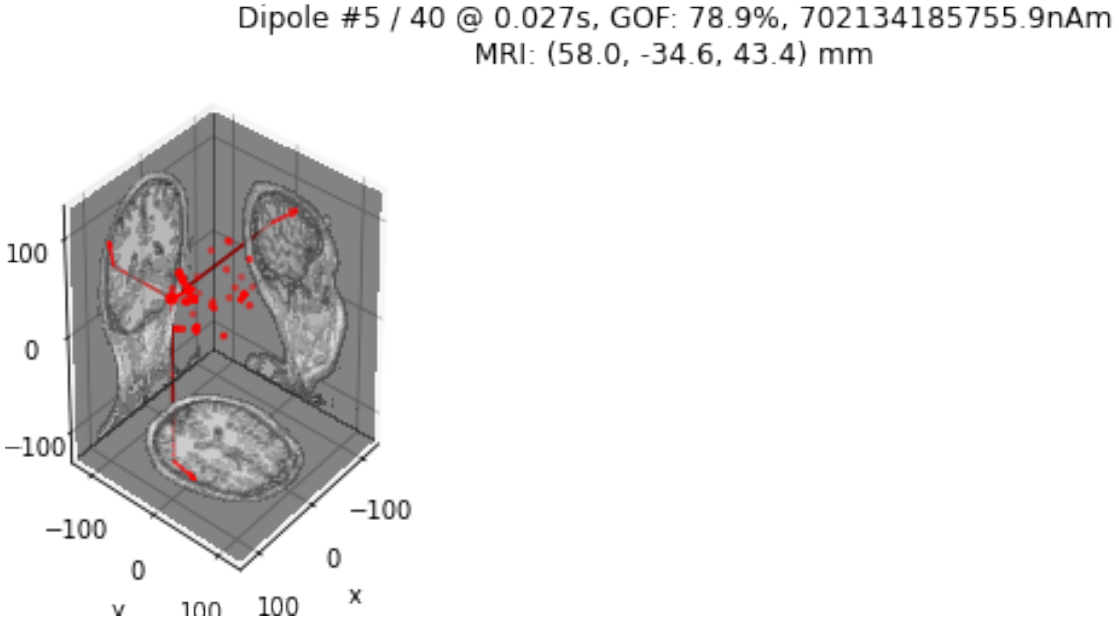

Figure 4: The figure represents the atoms mapped inside the brain using a dipole that has been fitted on the atoms **with the rank1 constraint** on the sample dataset [1]. Fiting a dipole allows to get closer to the true origin of the signal in the brain.

Algorithm 1: Locally greedy coordinate descent (LGCD)

Input : Signal X, atoms D_k, number of segments M, stopping parameter $\epsilon > 0$, z_k initialization
Initialize $\beta_k[t]$ with (5).
repeat
  for $m = 1$ **to** M **do**
    Compute $z'_k[t] = \max\left(\frac{\beta_k[t] - \lambda}{\|D_k\|_2^2}, 0\right)$ for $(k, t) \in \mathcal{C}_m$
    Choose $(k_0, t_0) = \underset{(k,t) \in \mathcal{C}_m}{\arg\max} |z_k[t] - z'_k[t]|$
    Update β with (6)
    Update the current point estimate $z_{k_0}[t_0] \leftarrow z'_{k_0}[t_0]$
until $\|z - z'\|_\infty < \epsilon$

Figure 5: Pseudo-code for the Locally greedy coordinate descent (LGCD) algorithm